Large electrocaloric effects in single-crystal ammonium sulphate

S. Crossley[1], W. Li[2], X. Moya[1] and N. D. Mathur[1*]

[1]Materials Science, University of Cambridge, Cambridge, CB3 0FS, United Kingdom

[2]School of Physics, Huazhong University of Science and Technology, Wuhan 430074, China

*ndm12@cam.ac.uk

Electrocaloric effects are typically studied near phase transitions in ceramic and polymer materials. Here we investigate electrocaloric effects in an inorganic salt, namely ammonium sulphate $(NH_4)_2SO_4$, with an order-disorder transition whose onset occurs at 223 K on cooling. For a single crystal thinned to 50 μm, we use a Maxwell relation to find a large isothermal entropy change of 30 J K^{-1} kg^{-1} in response to a field change of 400 kV cm^{-1}. The Clausius-Clapeyron equation implies a corresponding adiabatic temperature change of 4.5 K.

1. Introduction

Reversible electric-field-driven thermal changes are known as electrocaloric (EC) effects, and have been proposed for solid-state cooling applications. They peak at finite temperatures near ferroelectric and ferrielectric phase transitions, and are typically parametrised in terms of isothermal entropy change ΔS and the corresponding adiabatic temperature change ΔT. Ceramic oxides such as $PbSc_{0.5}Ta_{0.5}O_3$ [1-3] show first-order ferroelectric phase transitions that are traditionally considered to be displacive, implying relatively small entropic changes when applying 10s of kV cm^{-1}. In sub-micron-thick films of these materials, EC effects are enhanced because one may apply 100s of kV cm^{-1} without breakdown [4]. Somewhat larger EC effects are seen near order-disorder phase transitions in few-micron-thick polymer films, but these require larger fields of a few 1000 kV cm^{-1}

[5,6]. EC effects in both ceramic and polymer films could be exploited in multilayer capacitors to enhance active thermal mass [7-9], with active layer thicknesses of several microns [10-12] or 10s of microns [13]. Here we report large EC effects in a 50 μm-thick single-crystal of the inorganic salt ammonium sulphate (AS) [$(NH_4)_2SO_4$], using a moderate field of 400 kV cm^{-1}.

AS displays a predominantly order-disorder ferrielectric phase transition and thus a large thermally driven zero-field entropy change $|\Delta S| \sim 133$ J K^{-1} kg^{-1} for the full transition that spans a wide range of temperatures [14,15]. Among known ferroelectrics, this value is exceeded only by certain halides [16]. More generally, most inorganic ferroelectric/ferrielectric salts show predominantly order-disorder transitions, such that the ordered state is destroyed above the Curie temperature T_C by the thermally activated randomisation of ionic positions. Each randomisation contributes an entropy of $R\ln(2) = 5.8$ J K^{-1} per mole of ionic groups ($R = 8.314$ J K^{-1} mol^{-1}), which corresponds to tens of J K^{-1} kg^{-1} for typical salts [15]. Despite these large entropy changes, the study of EC effects in inorganic salts is rare [17,18]. That said, large entropy changes of $|\Delta S| = 60$ J K^{-1} kg^{-1} were recently achieved near the ferrielectric transition in powdered AS using relatively small changes of pressure $|\Delta p| = 0.1$ GPa, i.e. barocaloric effects of giant strength [19].

The ferrielectric phase transition in AS involves the ordering of all three ionic groups [14]. On cooling, partial order results in a first-order ferrielectric transition at $T_C \sim 223$ K, followed by a continuous increase of order down to ~160 K [14,18-20]. Here, for a bulk sample thinned to 50 μm, we achieve relatively large electrically driven changes of entropy $|\Delta S| \sim 30$ J K^{-1} kg^{-1} with $|\Delta E| = 400$ kV cm^{-1}, as deduced from measurements of electrical polarization $P(E)$ that were dense in temperature, using the well-known indirect method [21] with Maxwell relation $(\partial S/\partial E)_T = (\partial P/\partial T)_E$. Adiabatic temperature changes of up to $|\Delta T| \sim 4.5$ K are inferred from the Clausius-Clapeyron equation.

2. Experimental methods

Samples were prepared by mixing one equivalent of sulphuric acid (>aq. 95%) and two equivalents of ammonium hydroxide (aq. 35%) in water. The resultant white precipitate was dissolved in excess water, and kept at room temperature over a few days to yield transparent crystals of mixed morphologies. Small crystals (<1 mm^3) were used for X-ray diffraction, and larger crystals (several mm^3) were used for calorimetry and electrical measurements.

Temperature-dependent X-ray diffraction (performed using an Oxford Diffraction Gemini E Ultra, with Oxford Instruments Cryojet) confirmed the presence of a single phase with the expected lattice parameters [22], and revealed the presence of twins in the low-temperature phase.

Calorimetry was performed on an unelectroded crystal of mass 9.429 mg, using a TA Instruments Q2000 differential scanning calorimeter to measure heat flow while ramping temperature T at ± 2 K min^{-1}. As shown in [23], the resulting plots of $c(T)$ on cooling and heating were shifted to remove the offset in c away from T_C. The zero-field entropy change with respect to the absolute entropy at 230 K was evaluated from $c(T)$ using $\left|\Delta S_{230}(T)\right| = \left|\int_{230\mathrm{K}}^{T} c(T')/T' \,\mathrm{d}T'\right|$.

For dielectric and electrical polarization measurements, a single sample was prepared from a large crystal, as described in [23] and summarized here. The polar c-axis was identified by room-temperature X-ray diffraction using a Bruker D8 Advance. A surface lying normal to this direction was polished flat, covered with a bottom electrode of sputter-deposited Pt, and glued with conducting silver epoxy to insulating Kapton tape on a Cu substrate. The free surface was then polished flat, resulting in an AS thickness of ~50 μm, as measured in an optical microscope by focussing on the lower and upper surfaces of the transparent crystal and assuming a refractive index

of 1.53 [24]. A smaller top electrode of Pt was sputter deposited through a bespoke lift-off mask, and its ~0.5 mm^2 area was assumed to represent the electrically active area, ignoring fringing fields. Wiring was attached using epoxy glue, and vacuum grease (Apiezon 'n') was liberally smeared over the samples to discourage electrical arcing.

Dielectric measurements were performed using an Agilent 4294A Impedance Analyzer, with excitation amplitude 0.5 V and frequency 1 kHz. Temperature was ramped slowly at -0.2 K min^{-1} using an evacuated probe in liquid nitrogen, with a Cu heat reservoir and PID temperature control [23]. At all measurement temperatures, a constant parasitic parallel capacitance of 1.8 pF was subtracted from the measured capacitance, yielding a sample capacitance of 0.4 pF at 298 K. Subsequent temperature sweeps yielded a stable dielectric response, which was smaller than the response obtained during the initial sweep, due to some degree of cracking and degradation associated with the large and abrupt volume change at T_C [19 and references therein].

Electrical polarisation measurements of the same sample were obtained with a Radiant Precision Premier II and an external Trek amplifier, using a triangular wave excitation with period 0.1 s and amplitude 2 kV. The aforementioned probe was used to ramp temperature slowly at -0.1 K min^{-1}, in order to collect a dense set of polarization loops every ~0.07 K. Polarization data were noisy after correcting for a relatively large parasitic capacitance. An additional correction for temperature-independent high-field resistive losses (Supplementary Fig. 1) had no influence on $(\partial P/\partial T)_E$ and the resulting values of $\Delta S(E,T)$. A second sample measured with coaxial cable showed no such losses [23], which implies negligible Joule heating in direct measurements and any practical applications.

3. Results

For our unclamped sample, the first-order structural transition near T_C (Fig. 1a) is accompanied by a large peak in $c(T)$ and thus a large zero-field entropy change of $|\Delta S_0| \sim 50$ J K^{-1} kg^{-1} (Fig. 1b), with start and finish temperatures that from $c(T)$ we identify to be $T_{c1} = 221.9$ K and $T_{c2} = 221.1$ K. The other notable feature in $c(T)$ is that the background value of 1.5 kJ K^{-1} kg^{-1} near and below T_C is enhanced with respect to the background value of 0.9 kJ K^{-1} kg^{-1} near and above T_C, as a consequence of the transition extending below T_C [19]. The ferrielectric transition is also seen in dielectric data obtained for the virgin sample (Fig. 1c), where the $\varepsilon \sim 80$ peak in relative permittivity corresponds to the first-order transition. Further order on further cooling increases the very small high-temperature loss to a large value at 200 K, where $\tan \delta \sim 0.2$.

Electrical polarization loops for our clamped sample were noisy (Fig. 2), but below T_C it is possible to discern that the low-field rise in P is followed by a further step near $E \sim 200$ kV cm^{-1}, perhaps seen better in plots of $|P(T)|$ (Fig. 3a) that were obtained every $E \sim 5$ kV cm^{-1} by spline fitting to data from all ~276 $P(E)$ loops (selected spline fits appear in Fig. 4). This further step in $P(E)$ is associated with ferrielectric sublattice switching, yielding triple loops that were clearly resolved in Fig. 1b of [18]. Above T_C, the high-field step can also be detected, but it is not preceded by the low-field rise in P, implying the double loop associated with driving a transition above T_C [23,25,26].

In order to quantify EC effects in our clamped sample of AS, we first used our smoothed $|P(T,E)|$ dataset (Fig. 3a) to obtain $|(\partial P/\partial T)_E|$ in (E,T) space (Fig. 3b). From these data, we obtained the isothermal entropy change $\left|\Delta S(E)\right| = \left|\int_0^E \left(\partial P / \partial T\right)_{E'} \mathrm{d}E'\right|$ (Fig. 3c) due to the application or removal of field E, using Maxwell relation $(\partial S/\partial E)_T = (\partial P/\partial T)_E$ and density 1.770 g cm^{-3} [27]. We see that large EC effects with peak value of $|\Delta S| \sim 30$ J K^{-1} kg^{-1} may be driven by $|\Delta E| = 400$ kV cm^{-1} in a ~5 K temperature range.

4. Discussion

The EC effects that we have observed near the first-order transition in ferrielectric AS were conventional, but inverse EC effects are expected at lower temperatures given that further cooling implies further ferrielectric ordering [19] and thus a fall of spontaneous polarization [20], not seen in our narrow temperature range of measurement. The maximum applied field of 400 kV cm^{-1} is large for a sample thickness of 50 μm: it is far larger than all fields previously applied to AS [14,18,28]; larger than the 105 kV cm^{-1} that could be applied across a 38 μm-thick ceramic film [29]; and comparable with the fields used to achieve large EC effects in sub-micron-thick ceramic films.

The mass-normalized EC effects of $|\Delta S| \sim 30$ J K^{-1} kg^{-1} in our 50 μm-thick sample are only by a small factor smaller than those seen in much thinner micron-thick polymer films of similar density [5,6], where $|\Delta S| \sim$ 60-130 J K^{-1} kg^{-1} [21]. This implies an order of magnitude improvement in the entropy change for a given sample. Moreover, our mass-normalized EC effects are somewhat larger than the typical range of values obtained for bulk and thin-film ceramics, where $|\Delta S| \sim$ 1-10 J K^{-1} kg^{-1} [21]. Alternatively, we may note that the corresponding volume-normalized entropy change of 53 kJ K^{-1} m^{-3} exceeds the typical values for bulk ceramics by a small factor, and is comparable with the values obtained for thin ceramic films [21].

In order to convert our maximum isothermal entropy change $|\Delta S|$ into an adiabatic temperature change $|\Delta T|$ for our clamped sample of AS, we cannot use the heat capacity $c(T)$ data for unclamped AS (Fig. 1b) to construct adiabats [23,26]. However, AS powder possesses a 7 K transition width that is similar to the 5 K transition width for our clamped crystal, and therefore we may use the powder value of $c = 1.2$ kJ K^{-1} kg^{-1} at 223 K to deduce $|\Delta T| = 5.6$ K for our clamped crystal.

A better estimate of $|\Delta T|$ may be obtained via the Clausius-Clapeyron equation for the gradient $dE/dT_0 = -\rho\Delta S_0/\Delta P_0$ of the first-order phase boundary in (E,T) space, where the small value of $|\Delta P_0| \sim 1$ μC cm^{-2} (Fig. 3a) and the large value of $|\Delta S_0| \sim 50$ J K^{-1} kg^{-1} (Fig. 1b) represent the changes of polarisation and entropy across the full transition. The large resulting value of $|dE/dT_0| = 88$ kV cm^{-1} K^{-1} vastly exceeds the 1 kV cm^{-1} K^{-1} obtained for $PbSc_{0.5}Ta_{0.5}O_3$ with larger $|\Delta P_0| \sim 25$ μC cm^{-2} and smaller $|\Delta S_0| \sim 3.13$ J K^{-1} kg^{-3} [23,26]; is slightly larger than the 38 kV cm^{-1} K^{-1} that we tentatively read from the short phase boundary that changes by ~150 kV cm^{-1} in ~4 K (Fig. 3a); and implies that our 400 kV cm^{-1} field change should shift transition temperature T_0 by 4.5 K. This shift corresponds directly to an adiabatic temperature change $|\Delta T| = 4.5$ K, of the same order of manitude as the 5.6 K deduced in the previous paragraph.

5. Summary

We have reported large EC effects of $|\Delta S| = 30$ J K^{-1} kg^{-1} and $|\Delta T| = 4.5$ K when applying 400 kV cm^{-1} to a 50 μm-thick single crystal of AS, whose transition width was smeared by clamping from ~2 K (Fig. 1b) to ~5 K (Fig. 3). As discussed above, the mass-normalized entropy change reported here is only a small factor less than the values reported for much thinner polymer films, and it is larger than the values reported for bulk and thin-film ceramics.

In future, one might hope to achieve even larger EC effects in AS, given a value of $|\Delta S_0| \sim 50$ J K^{-1} kg^{-1} for the first-order component of the transition in an unclamped sample (Fig. 1b). Alternatively, large entropy changes of $|\Delta S| = 60$ J K^{-1} kg^{-1} can be achieved at $T = 219$ K by subjecting AS powder to changes of hydrostatic pressure [19]. Using the value of $c = 1.7$ kJ K^{-1} kg^{-1} for the powder at this temperature implies a correspondingly large value of $|\Delta T| = (T/c)|\Delta S| = 8$ K.

Overall, we have seen that the order-disorder nature of the ferrielectric transition in AS yields a large entropy change per sample. However, the large entropy change combined with the small ferrielectric polarization implies that large fields are required to achieve the large EC effects, as also seen for polymer films [5,6] by considering the field required to shift T_0 in the Clausius-Clapeyron equation $dT_0/dE = -\Delta P_0/\rho\Delta S_0$. In future, we hope that our findings will inspire EC studies in other order-disorder crystals, with enhanced values of $|\Delta P_0|$, and perhaps a value of $|\Delta S_0|$ that represents a compromise between EC effects ΔS and their strength $\Delta S/\Delta E$. It would also be attractive to develop cryogenic micro-thermometry and perform direct EC measurements.

Acknowledgements

We thank Thirumurugan Alagarsamy for fabricating the sample, and Robert Cornell for performing calorimetry experiments. X.M. is grateful for support from the Royal Society. W.L. acknowledges financial support from NSFC (Grant No. 21571072 and 61138006).

References

[1] X. Moya, E. Stern-Taulats, S. Crossley, D. González-Alonso, S. Kar-Narayan, A. Planes, Ll. Mañosa and N. D. Mathur. *Adv. Mat.* **25** 1360 (2013).

[2] L. A. Shebanov, E. H. Birks and K. J. Borman. *Ferroelectrics* **90** 165 (1989).

[3] B. Tuttle and D. Payne, *Ferroelectrics* **37** 603 (1981).

[4] A. S. Mischenko, Q. Zhang, J. F. Scott, R. W. Whatmore and N. D. Mathur, *Science* **311**, 1270 (2006).

[5] B. Neese, B. Chu, S,-G. Lu, Y. Wang, E. Furman and Q. M. Zhang, *Science* **321** 821 (2008).

[6] S. G. Lu, B. Rožič, Q. M. Zhang, Z. Kutnjak, Xinyu Li, E. Furman, L. J. Gorny, M. Lin, B. Malič, M. Kosec, R. Blinc and R. Pirc. *Appl. Phys. Lett.* **97** 162904 (2010).

[7] S. Kar-Narayan and N. D. Mathur, *Appl. Phys. Lett.* **95** (2009) 242903.

[8] R. I. Epstein and K. J. Malloy, *J. Appl. Phys.* **106** 064509 (2009).

[9] D. Guo, J. Gao, Y.-J. Yu, S. Santhanam, A. Slippey, G. K. Fedder, A. J. H. McGaughey, and S.-C. Yao, *Int. J. Heat. Mass. Trans.* **72** 559 (2014).

[10] S. Kar-Narayan and N. D. Mathur, *J. Phys. D: Appl. Phys.* **43** 032002 (2010).

[11] Y. Bai, G.-P. Zheng, K. Ding, L. Qiao, S.-Q. Shi, and D. Guo, *J. Appl. Phys.* **110** 094103 (2011).

[12] H. Gu, X. Qian, X. Li, B. Craven, W. Zhu, A. Cheng, S. C. Yao and Q. M. Zhang, *Appl. Phys. Lett.* **102** 122904 (2013).

[13] S. Hirose, T. Usui, S. Crossley, B. Nair, A. Ando, X. Moya and N. D. Mathur, *APL Materials*, submitted.

[14] S. Hoshino, K. Vedam, Y. Okaya and R. Pepinsky, *Phys. Rev.* **112** 405 (1958).

[15] J. F. Scott, *J. Phys. Soc. Japan* **58** 4487 (1989).

[16] H. Chihara and A. Inaba, *J. Chem. Thermodynamics*, **8**, 915 (1976).

[17] H. von Baumgartner, *Helv. Phys. Acta* **23** 651 (1950).

[18] S. Sawada, T. Yamaguchi and N Shibayama, *J. Phys. Soc. Japan* **48** 1395 (1980).

[19] P. Lloveras, E. Stern-Taulats, M. Barrio, J.-Ll. Tamarit, S. Crossley, W. Li, V. Pomjakushin, A. Planes, Ll. Mañosa, N. D. Mathur and X. Moya, *Nat. Comm.* **6** 8801 (2015).

[20] H. G. Unruh, *Sol. Stat. Comm.* **8** 1951 (1970).

[21] X. Moya, S. Kar-Narayan and N. D. Mathur, *Nature Materials* **13** 439 (2014).

[22] I. M. Shmyt'ko, N. S. Afonikova and V. I. Torgashev, *Phys. Sol. Stat.* **44** 2309 (2002)

[23] S. Crossley, PhD thesis, *University of Cambridge* (2013). Available at: http://www.repository.cam.ac.uk/handle/1810/245063.

[24] V. Y. Stadnyk, M. O. Romanyuk, B. V. Andrievskii, and N. R. Tuzyak, *Crystallogr. Rep.* **54** 313 (2009).

[25] W. J. Merz, *Phys. Rev.* **91** 513 (1953).

[26] S. Crossley, B. Nair, R. W. Whatmore, X. Moya and N. D. Mathur, manuscript in preparation.

[27] *Handbook of Chemistry and Physics*. Taylor & Francis, 94th ed., 2013.

[28] A. Sawada, S. Ohya, Y. Ishibashi and Y. Takagi, *J. Phys. Soc. Japan* **38** 1408 (1975).

[29] S. Crossley, T. Usui, B. Nair, S. Kar-Narayan, X. Moya, S. Hirose, A. Ando and N. D. Mathur, *Appl. Phys. Lett.* **108** 032902 (2016).

Figure Captions

Figure 1. Zero-field 223 K phase transition in AS observed on reducing temperature. (a) Lattice parameters. (b) Specific heat capacity c, and hence entropy change ΔS_{230} with respect to absolute entropy at 230 K. (c) Relative dielectric constant ε, and tan δ.

Figure 2. Electrical polarisation P versus electric field E for AS, on cooling.

Figure 3. EC properties of AS. (a) $P(E,T)$ obtained from upper ($E > 0$) and lower ($E < 0$) branches of ~350 $P(E)$ loops, some of which are shown in Fig. 2. (b) The resulting plot of $(\partial P/\partial T)_E$. (c) Isothermal entropy change $\Delta S(E,T)$ deduced from (b) using Maxwell relation $(\partial S/\partial E)_T = (\partial P/\partial T)_E$.

Figure 4. EC properties of AS plotted in the traditional manner. The information presented in Figure 3 is replotted here, for selected values of field E. In panel (a), we show data along with the corresponding spline fits (black curves).

Figure 1

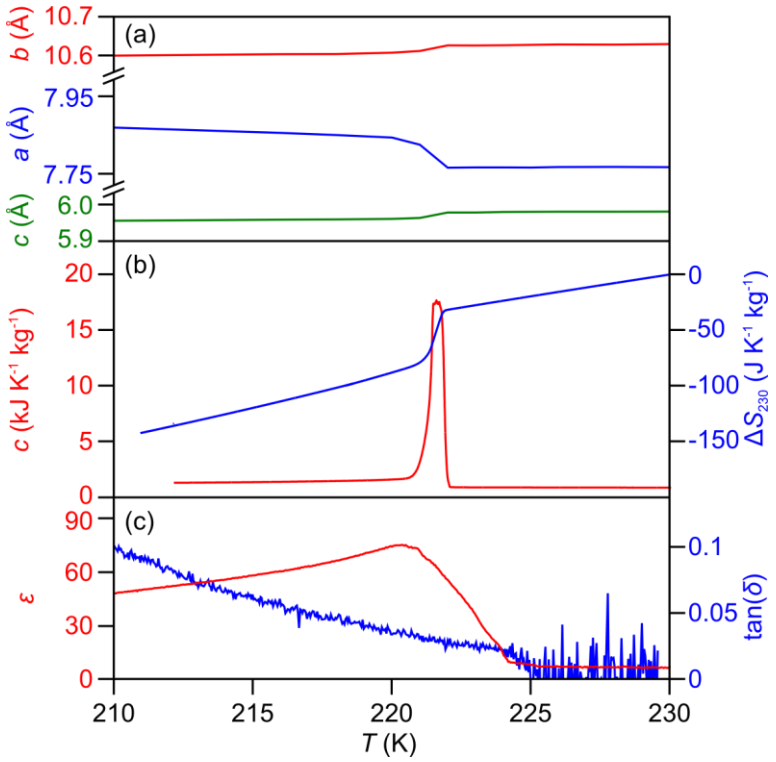
(a)
b (Å)
10.7
10.6
a (Å)
7.95
7.75
c (Å)
6.0
5.9
(b)
c (kJ K-1 kg-1)
20
15
10
5
0
ΔS230 (J K-1 kg-1)
0
-50
-100
-150
(c)
ε
90
60
30
0
tan(δ)
0.1
0.05
0
210
215
220
225
230
T (K)

Figure 2

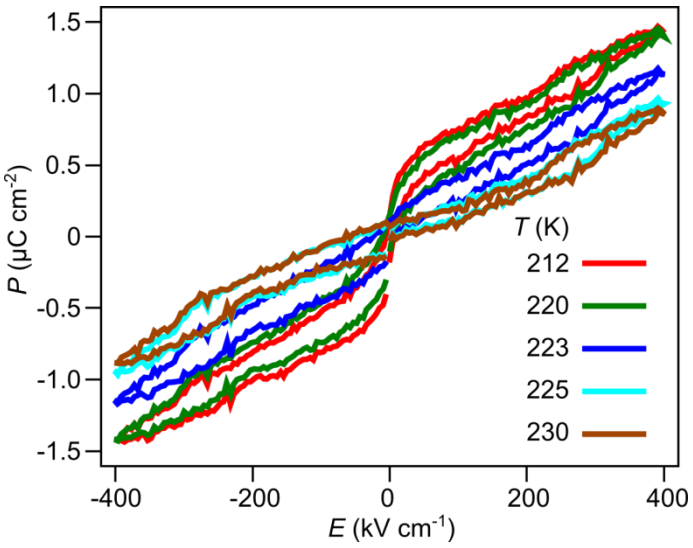
1.5
1.0
0.5
0
-0.5
-1.0
-1.5
P (μC cm-2)
-400
-200
0
200
400
E (kV cm-1)
T (K)
212
220
223
225
230

Figure 3

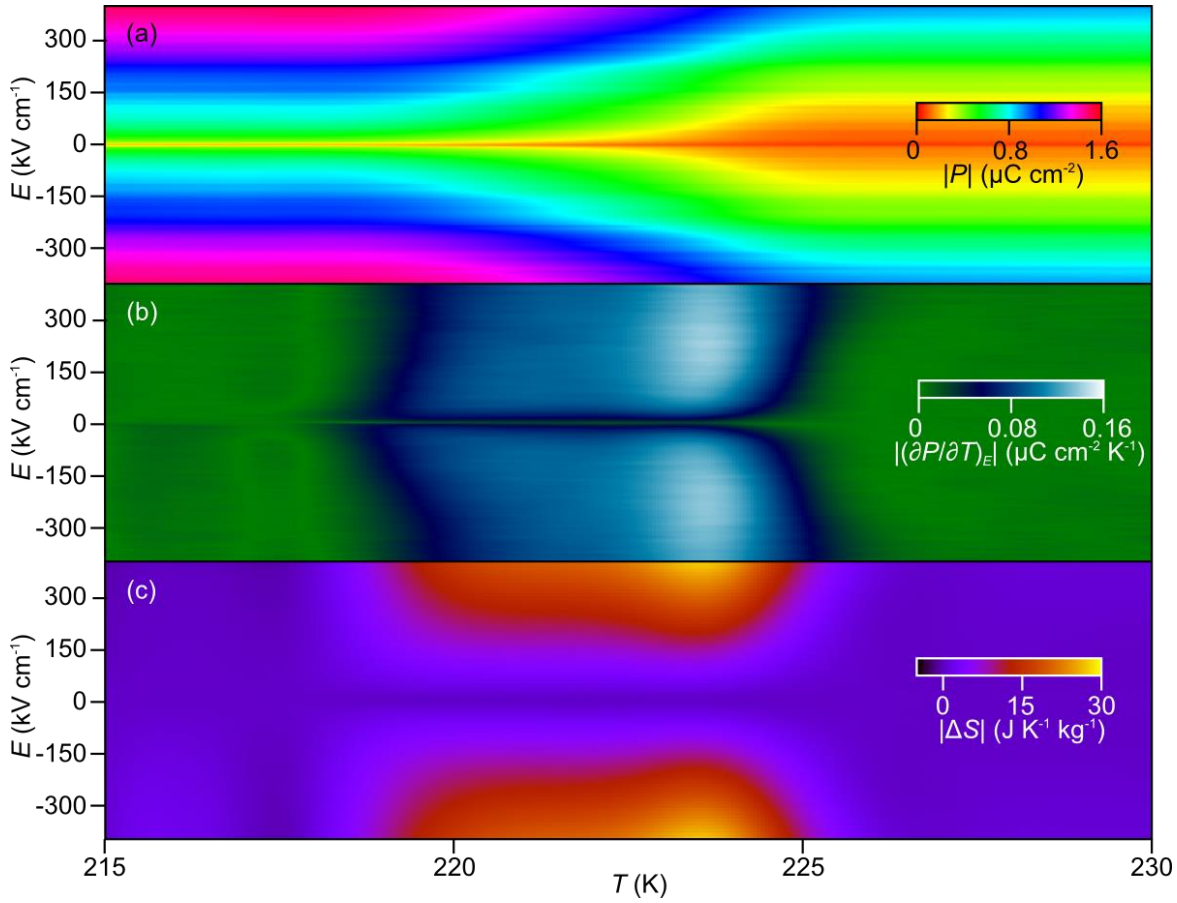
(a)
(b)
(c)
E (kV cm-1)
300
150
0
-150
-300
0
0.8
1.6
|P| (μC cm-2)
0
0.08
0.16
|(∂P/∂T)E| (μC cm-2 K-1)
0
15
30
|ΔS| (J K-1 kg-1)
215
220
225
230
T (K)

Figure 4

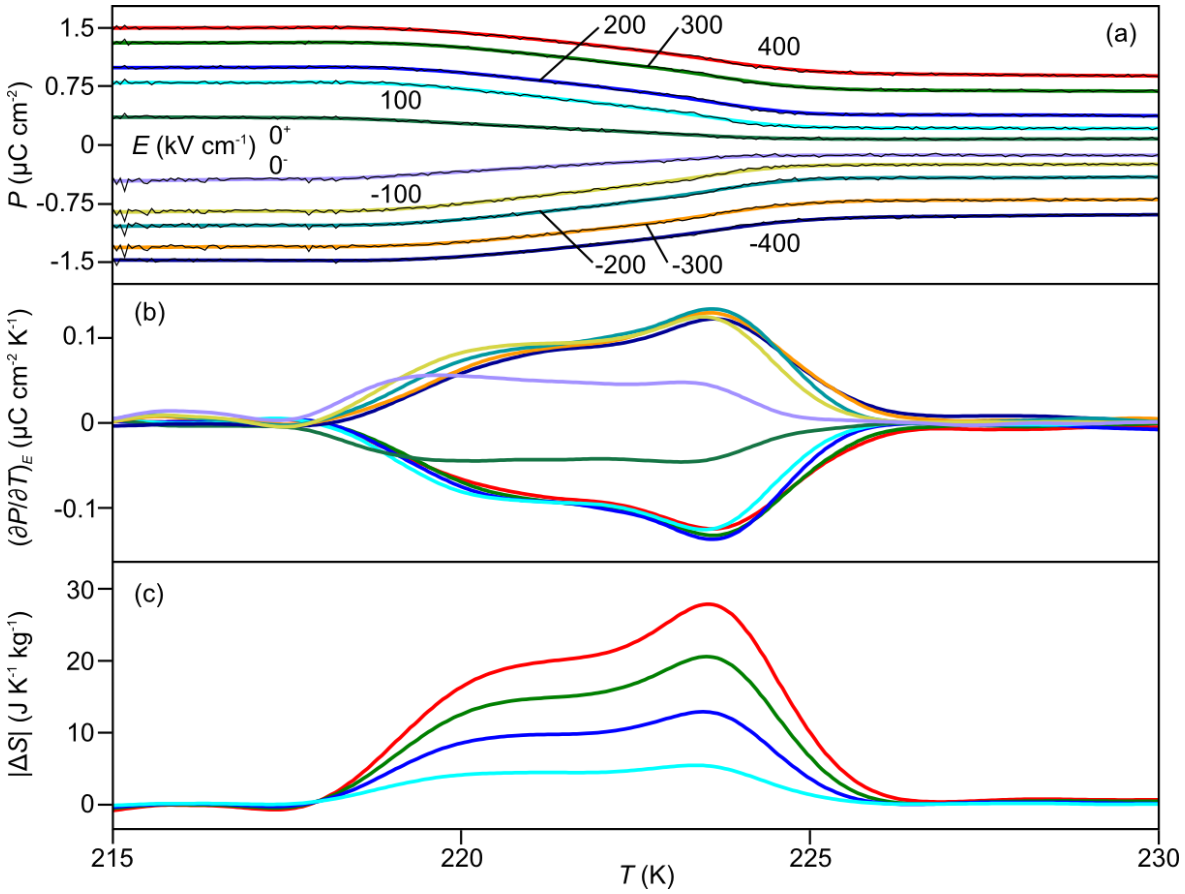
(a)
(b)
(c)
200
300
400
100
E (kV cm-1) 0+
0-
-100
-200
-300
-400
P (μC cm-2)
(∂P/∂T)E (μC cm-2 K-1)
|ΔS| (J K-1 kg-1)
T (K)
1.5
0.75
0
-0.75
-1.5
0.1
-0.1
30
20
10
215
220
225
230

Supplementary Information

for

Large electrocaloric effects in single-crystal ammonium sulphate

S. Crossley[1], T. Alagarsamy[1], W. Li[1], X. Moya[1], A. K. Cheetham[1] and N. D. Mathur[1*]

[1]Materials Science, University of Cambridge, Cambridge, CB3 0FS, United Kingdom

*ndm12@cam.ac.uk

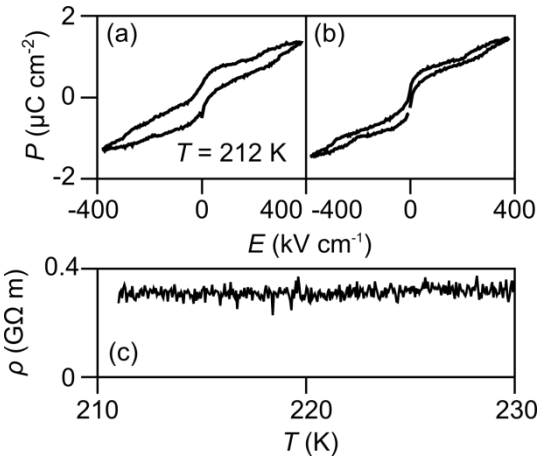

Supplementary Figure 1. Electrical loss correction. (a) A measured $P(E)$ loop, and (b) the same loop after compensating for losses associated with (c) the temperature-independent resistivity ρ = 0.4 GΩ m, which was measured at 400 kV cm^{-1} via the closure failure of unipolar $P(E)$ loops (raw data and methodology are described in S. Crossley, PhD thesis, *University of Cambridge* (2013)*). The same compensation was applied to all loops, and therefore does not affect the resulting values of pyroelectric coefficient $(\partial P/\partial T)_E$ used to evaluate isothermal entropy change $\Delta S(E,T)$.

*Available at: http://www.repository.cam.ac.uk/handle/1810/245063.